Document downloaded from http://www.elsevier.es, day 19/10/2018. This copy is for personal use. Any transmission of this document by any media or format is strictly prohibited.

J MATER RES TECHNOL. 2018;7(3):371–375

Available online at www.sciencedirect.com

jmr&t Journal of Materials Research and Technology

www.jmrt.com.br

Original Article

Development of a magnetic sensor for detection of moderate carburization damages in heat-resistant HP-Nb tubes of steam reforming furnaces☆

Juan E.C. Lopez[a,b], *Mónica P. Arenas*[a,b,*], *Clara J. Pacheco*[b], *Fábio S. Queiroz*[a], *Carlos B. Eckstein*[c], *Laudemiro Nogueira*[c], *Luiz H. de Almeida*[a], *João M.A. Rebello*[a], *Gabriela R. Pereira*[a,b]

[a] *Department of Metallurgical and Materials Engineering – Federal University of Rio de Janeiro, Rio de Janeiro, Brazil*
[b] *Laboratory of Nondestructive Testing, Corrosion and Welding (LNDC/COPPE) – Federal University of Rio de Janeiro, Rio de Janeiro, Brazil*
[c] *Petrobras, Rio de Janeiro, Brazil*

ARTICLE INFO

Article history:
Received 20 November 2017
Accepted 10 June 2018
Available online 25 July 2018

Keywords:
Carburization
Steam Reformer tubes
FEM simulation
Magnetic sensor

ABSTRACT

Although carburization is not a typical occurrence in steam reforming furnaces, this localized damage can occur and its detection is an important issue. A magnetic sensor based in the magnetic flux density variation has been proposed for the carburization detection in samples coming from steam reformer tubes. A three-dimensional model, by finite-element method (FEM), supported the optimization and development of a magnetic sensor for the detection of carburized samples. The experimental results indicated that the developed sensor, with high sensitivity, allowed to detect regions with moderate carburization damages.

© 2018 Brazilian Metallurgical, Materials and Mining Association. Published by Elsevier Editora Ltda. This is an open access article under the CC BY-NC-ND license (http://creativecommons.org/licenses/by-nc-nd/4.0/).

1. Introduction

Heat-resistant austenitic stainless steels are frequently used in petrochemical industry, especially in pyrolysis and steam reformer furnace tubes being exposed to temperature ranging between 600 and 1000 °C [1,2]. Particularly, for the steam reformer furnaces, the main failure mechanism is creep. However, in rare cases, moderate and localized carburization may occur at the inner wall of the tubes [3]. The presence of a carburized layer in these tubes can compromise their properties and affect their magnetic properties, interfering with the methodology for non-destructive inspection. Evaluation of these stem reformer tubes are usually performed during the maintenance shutdowns using non-destructive techniques such as the laser profilometry and eddy current testing to estimate their remaining life [4,5]. It has been

☆ Paper was part of technical contributions presented in the events part of the ABM Week 2017, October 2nd to 6th, 2017, São Paulo, SP, Brazil.

* *Corresponding author.*
E-mail: monica.correa@metalmat.ufrj.br (M.P. Arenas).

https://doi.org/10.1016/j.jmrt.2018.06.007

2238-7854/© 2018 Brazilian Metallurgical, Materials and Mining Association. Published by Elsevier Editora Ltda. This is an open access article under the CC BY-NC-ND license (http://creativecommons.org/licenses/by-nc-nd/4.0/).

Document downloaded from http://www.elsevier.es, day 19/10/2018. This copy is for personal use. Any transmission of this document by any media or format is strictly prohibited.

Table 1 – Chemical composition of the samples. HP-modified alloy (wt%).

Cr	Ni	C	Mn	Si	P	S	Mo	Co	Nb	Ti
26.1	34.3	0.52	1.26	1.89	0.023	0.012	0.018	0.061	1.26	0.010

also reported that the external surface presents a ferromagnetic response, being important to magnetically saturate it and thus, overpass this effect and measure the magnetic response of the carburized layer [6–10]. The carburization phenomenon occurs by the absorption of carbon at the inner tube wall, with the consequent precipitation of chromium carbides and depletion of the austenitic matrix in chromium content [11,12]. Below a critical chromium content, the austenite matrix exhibits a ferromagnetic behavior at room temperature [6], feature which allow to use magnetic sensors for the detection of carburization. Based on this statement, this work presents the development of a magnetic sensor to detect moderate carburization damages in HP tubes coming from steam reformer furnaces. Carburization damages are a common occurrence in pyrolysis furnaces. It has been reported magnetic sensors development to detect carburization up to 39% of the wall thickness [13]. However, in the present case of study, the samples present carburization up to 7.5% of the wall thickness, which requires the development of the magnetic sensor with high sensitivity in order to maximize the signal-to-noise ratio for detection of moderate and localized carburization damages.

A model simulation was developed in order to optimize the characteristics of the magnetic sensor. The simulation was performed in COMSOL Multiphysics® in which the geometry and the magnetic properties of the sensor were optimized. Thus, the magnetic sensor allowed to establish a correlation between the magnetic flux density and the presence of a carburized layer formed at the inner tube wall.

2. Materials and methods

2.1. Samples

Three samples were extracted at different heights from the same steam reformer tube, which was in service for 130,000 h. The outer diameter, thickness and length of the tested tubes are 134 mm, 16 mm and 200 mm, respectively. The chemical composition of the sample is shown in Table 1.

Metallographic samples were extracted from the tube cross-section for the analysis by microscopic and magnetic techniques. Table 2 shows the operating temperature of the steam reformer tube from which the samples were extracted. Metallographic samples were characterized by scanning electron microscopy (SEM) using the VEGA 3LMU TSCAN in the backscattered electron mode (BSE). The SEM analysis was performed close to the internal tube wall. The vibrating sample magnetometer was also used in order to obtain the magnetization curves along the tube thickness, on rectangular samples with 6 mm long and 1.5 mm wide and deep.

Table 2 – Operating temperatures of the samples.

Samples	Temperature (°C)
A	600
B	700
C	1000

The non-destructive evaluation was performed on the tube external wall. For each tube, the carburized region was removed in a depth of 1.5 mm along 60 mm in length. This procedure was used in order to compare the magnetic response in carburized and decarburized regions.

2.2. Development and optimization of the magnetic sensor

In literature has been reported the magnetic sensor development for detection of highly carburized pyrolysis wall tubes [7,8,13,14]. It is commonly used a magnetization coil to saturate the magnetic effect of the external surface and then, an eddy current sensor is used to measure the carburization damages [7,8,14]. However, magnetic techniques for nondestructive evaluation in steam reformer tubes with moderate carburization damages has not been reported. The analyzed samples exhibited a maximum percent of 7.5% of carburized wall thickness. Owing to this, it was necessary to implement a magnetic sensor with higher sensitivity. It was developed a compact magnetic sensor in which the loop is closed on the tube external surface in order to saturate its magnetic effect [9,10]. The sensor also allowed the detection of this moderate percent of carburization by using a Hall sensor positioned at its center. A computational simulation supported the sensor development, which allowed to optimize its geometry and magnetic properties. The simulation was performed in COMSOL Multiphysics® software by using a magnetostatic 3D model, which allowed to set the suitable parameters for building an optimal magnetic sensor.

3. Results

3.1. Microstructural characterization

The SEM analysis, using the backscattering electron detector (BSE), was performed close to the tube inner wall. As shown in Fig. 1, the sample C exhibits three different regions. On the left side is observed the bulk region (R1), followed by the carburized region (R2) and then, by a damaged zone (R3), composed by oxides and Fe-Ni. The bulk exhibits coarsened primary carbides and a fine secondary precipitation within the austenitic matrix. The sample with maximum carburized region presented a thickness of approx. 800 μm, which microstructure is characterized by a coarsened interdendritic precipitates and a massive secondary precipitation. The damaged zone extends radially for approx. 400 μm (darkest region).

Document downloaded from http://www.elsevier.es, day 19/10/2018. This copy is for personal use. Any transmission of this document by any media or format is strictly prohibited.

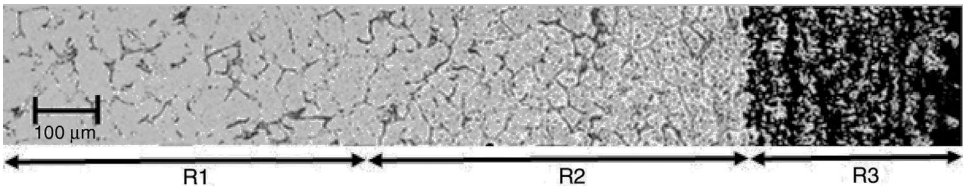

Fig. 1 – SEM micrograph (cross-section) of sample C exposed at 1000 °C showing three zones. On the left-side is observed the bulk, followed by the carburized region (800 µm) and the damaged zone (400 µm).

Table 3 – Thickness of carburized region and the damaged zone close to inner surface of the samples.

Samples	Carburized region (µm)	Damaged zone (µm)	Total (µm)
A	<50	0	<50
B	450	200	650
C	800	400	1200

Table 3 shows the measurements of the carburized regions and the damaged zones for the three studied samples. The damaged zone was taken into account for the total thickness measurement. It is observed that sample C presented the thickest carburized region.

3.2. *Magnetic characterization using the vibrating sample magnetometer (VSM)*

The model simulation was developed using the magnetic properties of sample C, due to present the thickest carburized layer. The magnetization curves were obtained by using the VSM LakeShore7400 model, by applying a magnetic field strength (*H*) in a range up to 500 mT. As shown in Fig. 2, when *H* is 500 mT, the external layer and carburized region presented a ferromagnetic behavior with magnetization of approx. 8 Am^2/kg and 18 Am^2/kg, respectively. The carburized layer exhibited the highest magnetic response, but no magnetic saturation is observed. In contrast, the external layer saturated at $H = 80$ mT. On the other hand, it is observed a paramagnetic response on the bulk. These

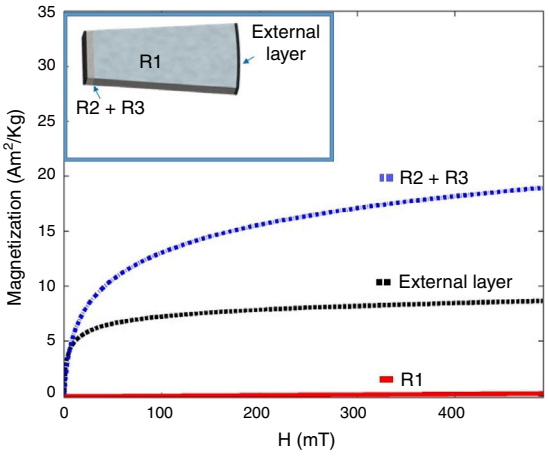

Fig. 2 – Magnetization curves performed on the tube external layer, bulk and carburized layer of sample C.

magnetization curves were used as inputs for the FEM simulation.

3.3. *Computational model*

As described on Section 2.2, the sensors reported in the literature is commonly used for detection of high carburization levels. However, the studied samples present up to 7.5% of wall thickness carburization, which requires the improvement of the magnetic sensor sensitivity, maximizing the signal-to-noise ratio for detection of moderate and localized carburization damages. For this reason, it was necessary to improve the geometry and avoid losses caused by magnetic flux leakages. In addition, the sensor geometry was adjusted until an optimal design model which guarantees the best coupling between the magnetic sensor and the sample.

A U-shaped core geometry (yoke) was taken into account to ensure the fit with the tube external wall, a tilt was also consider to guarantee a perfect coupling. In order to obtain results close to real values, the mesh was refined on the region of the magnets, on the carburized region and on the external surface, Fig. 3a. In the model was considered the use of a Hall sensor, element that allowed to measure magnetic variations in the experiments. For this model, tetrahedral elements were set with a minimum size of 0.06 mm. Fig. 3b shows the magnetic field density generated by the yoke, which is conducted through the entire sample thickness, switching the magnetic circuit. It is also observed a high magnetic flux density (above 500 mT) on the interface between the tube external wall and yoke, which ensures the magnetic saturation of the external layer [7,8]. Considering the operating range of the Hall sensor, it was required a bias in order to guarantee the linear operation of the magnetic sensor.

By using the post-processed results from the FEM simulation, it was observed that the magnetic flux density is almost the same on the tube external layer, as shown in Table 4. On the other hand, if compared the magnetic flux density on the internal tube wall, it is observed an increase of approx. 30% in the carburized sample.

3.4. *Results obtained with a magnetic sensor*

According to the model developed by computational simulation, the magnetic sensor was built, composed by a ferromagnetic U-shaped core, permanent magnets and a Hall sensor. The permanent magnets were placed at the core ends while the Hall sensor (MLX90242) was located at the U-shape core center. It guarantees that the Hall sensor is positioned on the axis of symmetry in order to reduce magnetic field losses. A magnetic bias was also used in

Document downloaded from http://www.elsevier.es, day 19/10/2018. This copy is for personal use. Any transmission of this document by any media or format is strictly prohibited.

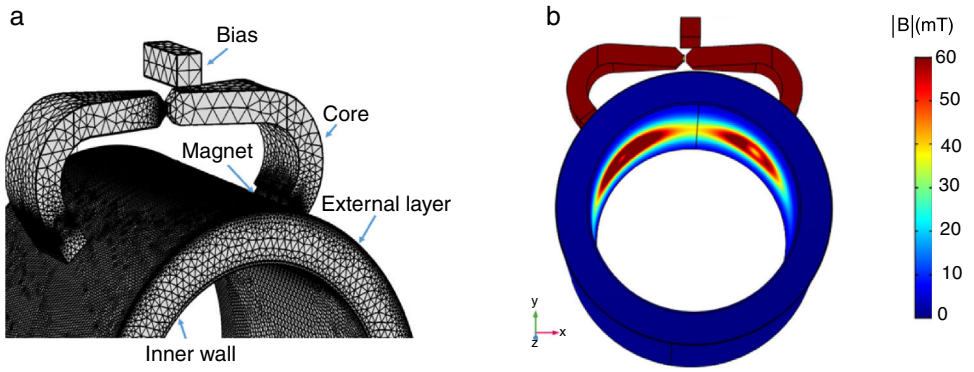

Fig. 3 – Magnetic sensor geometry (a) Mesh in the model geometry, (b) Magnetic flux density through-wall the carburized sample (closed magnetic circuit).

Table 4 – Magnetic flux density of sample D obtained by the FEM simulation. Results obtained in the internal and external tube wall.

Reference points	Decarburized region [mT]	Carburized region [mT]
Tube external layer	508.69	510.26
Inner tube wall	53.56	67.69

order to guarantee the linear operation of the Hall sensor in approximately ±40 mT. The Hall sensor was powered by +5 V and the output voltage was acquired using a multimeter. Once the magnetic sensor is approximated to the tested sample, it is created a closed loop, as showed in Fig. 3b. Thus, it was possible to establish a correlation between the magnetic sensor voltage and the carburization level. Each sample was tested in order to measure the magnetic response and then, compare the results performed in carburized and decarburized regions. Fig. 4 shows the output voltage obtained with the magnetic sensor according to carburization level in samples with and without carburization damages. Carburized samples exhibit an exponential tendency as a function of the carburization level. It is also observed that decarburized samples present a lower magnetic response. However, its magnetic response tends to increase, this behavior may be related to the influence of the external layer [9]. Thus, for each sample, it is observed an increase of approx. 60% in the carburized region in comparison with decarburized region.

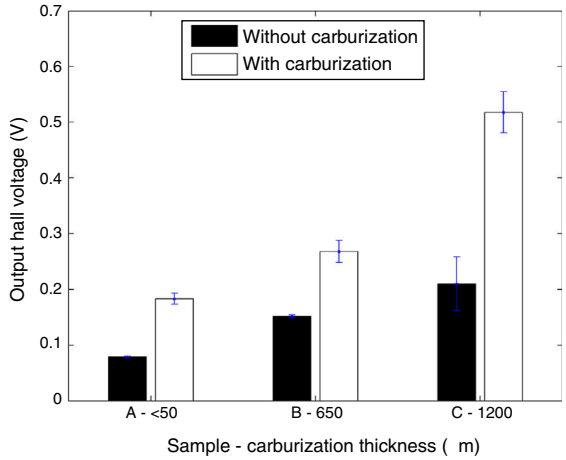

Fig. 4 – Output Hall voltage for samples with carburized and decarburized regions.

4. Discussion

The computational model allowed to optimize the geometry of the sensor and, thus, to avoid losses of magnetic flux when coupling the sensor on the tube external wall. In this way, a compact magnetic sensor was built in order to saturate the magnetic effect of the external surface and to detect the presence of moderate carburization damages, being a suitable system for the inspection in situ. The variation of the magnetic flux density, caused by the presence of different carburization contents, was measured by using a Hall sensor, positioned on the symmetry axis of the magnetic circuit. With the micrographs was established a correlation between the carburized thickness and the magnetic response, as shown in Fig. 4. Thus, if compared carburized and decarburized regions of the same sample, it is observed a reliably separation between both regions. The magnetostatic sensor presented high sensitivity and repeatability for detection of moderate carburization damages in HP steels, presenting higher sensitivity if compared to literature studies [7,8,13,14], in which high carburization damages were measured. However, the sensor developed is being able to detect even 0.05 mm of carburized and damaged region in samples with 16 mm of wall thickness.

5. Conclusion

A new magnetic sensor with higher sensitivity was built in order to detect moderate levels of carburization in HP steam reformer tubes. A finite element simulation allowed to observe the distribution of the magnetic flux density along the sample thickness and, consequently, supported the sensor enhancement for setting the optimal geometry and magnetic properties. The final prototype allowed to successfully detect internal carburized damages with detection sensitivity above 50 μm of the tube thickness.

Document downloaded from http://www.elsevier.es, day 19/10/2018. This copy is for personal use. Any transmission of this document by any media or format is strictly prohibited.

Conflicts of interest

The authors declare no conflicts of interest.

Acknowledgments

The authors would like to thank the Brazilian research agencies CAPES, CNPq, FAPERJ and FINEP for the financial support and Petrobras for supplying the samples.

REFERENCES

[1] Nunes FC, de Almeida LH, Dille J, Delplancke JL, Le May I. Microstructural changes caused by yttrium addition to NbTi-modified centrifugally cast HP-type stainless steels. Mater Charact 2007;58:132–42.

[2] da Silveira TL, Le May I. Reformer furnaces: materials, damage mechanisms and assessment. Arab J Sci Eng 2006;31:99–119.

[3] da Silveira TL, May ILM. Damage assessment and management in reformer furnaces. J Press Vessel Technol 1997;119:423–7.

[4] Roberts RD. Laser profilometry as a inspection method for reformer catalyst tubes. NDT Net 1999;4.

[5] Matesa B, Samardzic I, Bodenberger R, Sachs B, Pecic V. Eddy Current Inspection in Processing Furnace Remaining Life Prediction, Saf. Reliab. Welded Components Energy Process. Ind. 2. (n.d.) 359–64.

[6] Stevens KJ, Trompetter WJ. Calibration of eddy current carburization measurements in ethylene production tubes using ion beam analysis. J Phys D Appl Phys 2004;37:501–9.

[7] Kasai N, Ogawa S, Oikawa T, Sekine K, Hasegawa K. Detection of carburization in ethylene pyrolysis furnace tubes by a C core probe with magnetization. J Nondestruct Eval 2010;29:175–80.

[8] Hasegawa K, Oikawa T, Kasai N. Development of an eddy current inspection technique with surface magnetization to evaluate the carburization thickness of ethylene pyrolysis furnace tubes. J Nondestruct Eval 2012;31: 349–56.

[9] Pereira JMB, Pacheco CJ, Arenas MP, Araujo JFDF, Pereira GR, Bruno AC. Novel scanning dc-susceptometer for characterization of heat-resistant steels with different states of aging. J Magn Magn Mater 2017;442:311–8, http://dx.doi.org/10.1016/j.jmmm.2017.07.004.

[10] Arenas MP, Silveira RM, Pacheco CJ, Bruno AC, Araujo JFDF, Eckstein CB, Nogueira L, de Almeida LH, Rebello JMA, Pereira GR. Magnetic evaluation of the external surface in cast heat-resistant steel tubes with different aging states. J Magn Magn Mater 2018, http://dx.doi.org/10.1016/j.jmmm.2018.02.051.

[11] Tawancy HM, Abbas NM. Mechanism of carburization of high-temperature alloys. J Mater Sci 1992;27, https://link.springer.com/content/pdf/10.1007%2FBF01197661.pdf.

[12] Silva IC, Rebello JMA, Bruno AC, Jacques PJ, Nysten B, Dille J. Structural and magnetic characterization of a carburized cast austenitic steel. Scr Mater 2008;59: 1010–3.

[13] Khodamorad SH, Haghshenas DF. Inspection of carburization and ovalness in ethylene cracking tubes by using a semi-robot. Eng Fail Anal 2012;25:81–8, http://dx.doi.org/10.1016/j.engfailanal.2012.04.006.

[14] Stevens K, Tack A, Thomas C, Stewart D. Through-wall carburization detection in ethylene pyrolysis tubes. J Phys D Appl Phys 2001;34:814–22.